Macrophage M1/M2 Polarization Dynamically Adapts to Changes in Cytokine Microenvironments in *Cryptococcus neoformans* Infection

Michael J. Davis,[a] Tiffany M. Tsang,[a,b] Yafeng Qiu,[a] Jeremy K. Dayrit,[c] Joudeh B. Freij,[a] Gary B. Huffnagle,[a] Michal A. Olszewski[a,c]

Division of Pulmonary and Critical Care Medicine, University of Michigan, Ann Arbor, Michigan, USA[a]; Department of Molecular, Cellular and Developmental Biology, Yale University, Kline Biology Tower, New Haven, Connecticut, USA[b]; Veterans Affairs, Ann Arbor, Michigan, USA[c]

ABSTRACT **The outcome of cryptococcal pneumonia correlates with local macrophage polarization status, as M1 and M2 polarization marks protective and nonprotective responses, respectively. Overall, pulmonary macrophage polarization status changes over time during a cryptococcal infection. This could have been caused by repolarization of individual macrophages or by a replacement of M2-polarized cells by new M1-polarized cells. To explore the ability of macrophages to change between polarization states, we conducted a series of experiments using *in vitro* macrophages. Coculture of macrophages with *Cryptococcus neoformans* resulted in development of a weak M1-like phenotype, with modestly increased inducible nitric oxide synthase (iNOS) but lacking interleukin 6 (IL-6) induction. The *C. neoformans*-induced M1-like polarization state was plastic, as macrophages stimulated first with *C. neoformans* and then with gamma interferon (IFN-γ) or IL-4 expressed mRNA polarization patterns similar to those stimulated with cytokines alone. To further evaluate macrophage polarization plasticity, cytokine stimulatory conditions were established which fully polarized macrophages. IFN-γ and IL-4 stimulation differentially induced complete M1 and M2 polarization, defined by differential expression of marker mRNA panels, surface marker expression, and tumor necrosis factor alpha (TNF-α) protein production. Switching IFN-γ- to IL-4-stimulating conditions, and vice versa, resulted in uniform changes in profiles of polarization marker genes consistent with the most recent cytokine environment. Furthermore, the ability of sequentially stimulated macrophages to inhibit *C. neoformans* reflected the most recent polarizing condition, independent of previous polarization. Collectively, these data indicate that M1/M2 macrophage polarization phenotypes are highly plastic to external signals, and interventions which therapeutically repolarize macrophages could be beneficial for treatment of cryptococcosis.**

IMPORTANCE **Our studies reveal how a major opportunistic fungal pathogen, *Cryptococcus neoformans*, interacts with macrophages, immune cells which can ingest and kill invading pathogens. Macrophages play a crucial role in the pathogenesis of cryptococcal infection, as their polarization phenotype determines the outcome of the battle between the infected host and *C. neoformans*. This study suggests that dynamic changes in polarization of macrophages at the level of individual cells are an important characteristic of *in vivo* cryptococcosis, as they occur throughout the natural course of infection. We demonstrate that macrophages can rapidly and uniformly reverse their polarization phenotype in response to dynamic signaling conditions and lose or regain their fungicidal function. Demonstrating importance of these pathways may become a cornerstone for novel therapeutic strategies for treatment of cryptococcosis in both immunocompromised and immunocompetent patients.**

Received 9 April 2013 **Accepted** 20 May 2013 **Published** 18 June 2013

Citation Davis MJ, Tsang TM, Qiu Y, Dayrit JK, Freij JB, Huffnagle GB, Olszewski MA. 2013. Macrophage M1/M2 polarization dynamically adapts to changes in cytokine microenvironments in *Cryptococcus neoformans* infection. mBio 4(3):e00264-13. doi:10.1128/mBio.00264-13.

Editor Françoise Dromer, Institut Pasteur

Address correspondence to Michal A. Olszewski, olszewsm@umich.edu.

Cryptococcus neoformans is an opportunistic yeast pathogen and a leading cause of mortality in immunocompromised individuals. The yeast primarily infects the host lungs and subsequently disseminates into the central nervous system, where it can cause grave pathologies, including death (1–3). *C. neoformans* infection occurs most frequently in immunocompromised individuals, but a significant proportion of infections still occur in noncompromised individuals (4–6).

The clinical outcome of *C. neoformans* infection is highly dependent on the adaptive host immune response. In favorable circumstances, hosts mount a Th1-dominated immune response associated with high levels of gamma interferon (IFN-γ), resultant M1 macrophage polarization bias, and M1 macrophage-associated fungicidal activity (7–11). The antimicrobial properties of M1 macrophages are linked to upregulation of enzymes that generate microbicidal factors, including inducible nitric oxide synthase (iNOS) that generates nitric oxide from L-arginine (12–15).

In contrast, M2 macrophages are typically found in Th2-dominated responses (16, 17), as the Th2-driving interleukin 4 (IL-4) is a strong inducer of M2 polarization (7, 9, 18). During *C. neoformans* infections, the M2 cells cannot contain cryptococcal replication (9, 18, 19). One explanation is that the M2 cells do not upregulate iNOS but upregulate arginase (Arg-1), which uti-

lizes L-arginine via a nonfungicidal pathway. Other genes induced by M2 cells include the chitinase-like proteins Ym-1 and Ym-2 and Fizz (also called Relm-α) (20–22). Apart from the potential to harbor and propagate the *C. neoformans* in the infected host, the infected M2 might contribute to cryptococcal dissemination (11, 23–25). Thus, macrophages and their polarization status are the key factors in anticryptococcal defenses, which determine control versus progression of *C. neoformans* infection.

A recent study demonstrated that the lung immune polarization environment changes over time in a model of chronic *C. neoformans* infection using C57BL/6 mice (26). The *in vivo* cytokine profile in *C. neoformans*-infected lungs changed from an IL-4-dominated to an IFN-γ-dominated response over several weeks, with a corresponding shift in the overall macrophage polarization from M2 to M1 (26). The mechanism of this repolarization process is unknown. Whether the initially recruited and polarized macrophages can be repolarized in the target organ or need to be replaced by newly recruited/polarized cells is a subject of ongoing debate. Thus, we sought to determine if by changing the cytokine environment, M2-polarized macrophages could be diverted toward the M1 phenotype and regain their fungicidal potential. Our data show that *in vitro* macrophage polarization is phenotypically and functionally plastic in response to changing cytokine and fungus-sensing environments and that *in vitro* macrophage fungicidal potential is determined by the final stimulus independent of any previous stimulation.

RESULTS

***Cryptococcus neoformans* infection in BALB/c mice results in dynamic shifts in pulmonary macrophage polarization.** To determine if changes in macrophage polarization status were not uniquely restricted to the C57BL/6 mouse infection model (26), the kinetics of *in vivo* macrophage polarization were evaluated in BALB/c mice following intratracheal infection with 10^4 CFU of *C. neoformans* 24067. In this model, all BALB/c mice survive, and the clearance dynamics are well established (27–30). Briefly, *C. neoformans* expands to a high titer by week 1 (6.3 to 6.9 log CFU), plateaus at week 2, and is gradually cleared, reaching the initial inoculum level by week 6 (27, 28, 30). The mRNA expression of the primary M1 and M2 polarization markers, iNOS and Arg-1, was evaluated in adherence-enriched macrophages from *C. neoformans*-infected mouse lungs. At 1 week postinfection, the pulmonary macrophages were strongly M2 polarized, as they expressed high levels of Arg-1 mRNA and very low levels of iNOS mRNA (Fig. 1A and B). At 3 and 4 weeks postinfection, the overall polarization of macrophages shifted to M1 as iNOS expression increased and Arg-1 expression decreased (Fig. 1A and B). Finally, macrophage polarization appeared to be returning toward uninfected baseline at 5 weeks postinfection, with the expression levels of both marker genes as well as their relative ratio approaching baseline levels (Fig. 1A). Thus, at the population level, *in vivo* pulmonary macrophage polarization status evolves from resting to M2 polarization to M1 polarization and then back to resting levels (Fig. 1A and B).

***Cryptococcus neoformans* induces only weak macrophage polarization.** We next evaluated the direct effect of *C. neoformans* on *in vitro* M1/M2 macrophage polarization. For these studies, RAW 264.7 macrophages were incubated for 24 h with nonimmune mouse serum-opsonized or unopsonized live *C. neoformans* 208821 (15, 19, 31). Unopsonized cryptococci did not have any

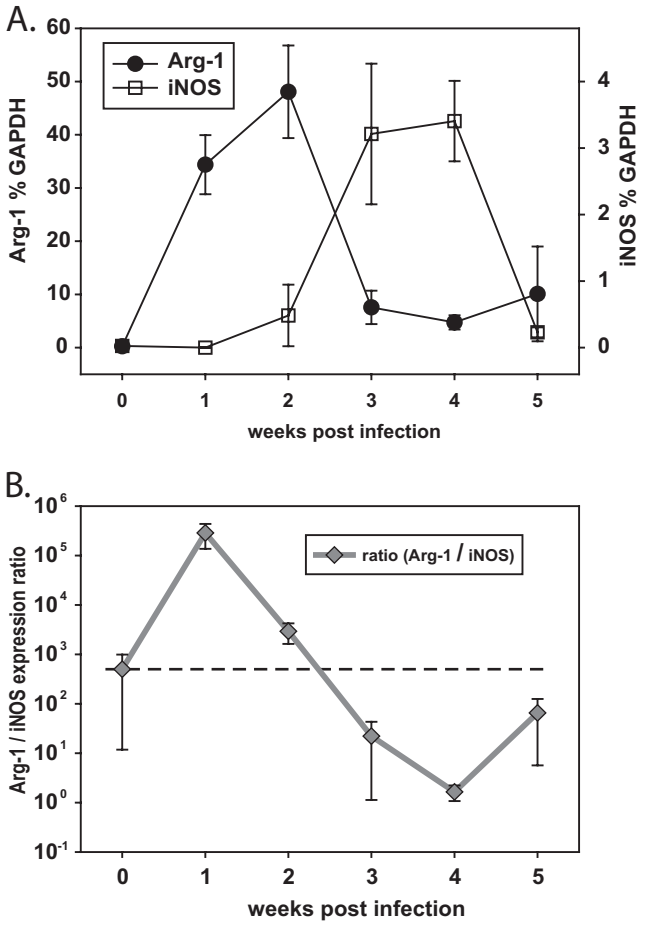

FIG 1 Macrophage polarization is dynamically altered during infection with *C. neoformans in vivo*. BALB/c mice were infected intratracheally with 10^4 live *C. neoformans* cells. Lung macrophages isolated at the indicated time points postinfection were analyzed by qPCR for mRNA expression of iNOS and Arg-1 genes, marker genes for M1 and M2 polarization, respectively. (A) A plot comparing the kinetics of Arg-1 and iNOS expression by pulmonary macrophages. Symbols indicate expression as average percent GAPDH. (B) A plot of the average ratio of Arg-1 expression to iNOS expression. The dashed line indicates the baseline expression ratio. In both plots, the symbols depict data from at least 4 mice per time point, and error bars denote SEMs. Note that the polarization of these macrophages evolves over time.

effect on expression of any macrophage polarization genes, even at higher multiplicities of infection (MOI). Serum opsonization resulted in a modest but dose-dependent induction of iNOS compared to that of unstimulated cell cultures (Fig. 2A), such that the effect was mostly visible at the highest dose of the yeast. This increased iNOS expression was not accompanied by any increased expression of the IL-6 M1 cytokine or the Arg-1 and Ym-2 M2 marker genes (Fig. 2A). These results were further validated in bone marrow-derived macrophages (BMM) pulsed with serum-opsonized *C. neoformans*. Consistent with the data in RAW cells, compared to unstimulated BMM there was a weak upregulation of iNOS in yeast-stimulated BMM which was much less than that induced by IFN-γ (Fig. 2B). Likewise, no change in IL-6 or Ym-2 expression was observed in *C. neoformans*-pulsed BMM. However, compared to unstimulated BMM, there was a weak upregulation of Arg-1 expression in yeast-stimulated BMM, which was much less than that induced by IL-4 (Fig. 2B). Thus, the 24-h

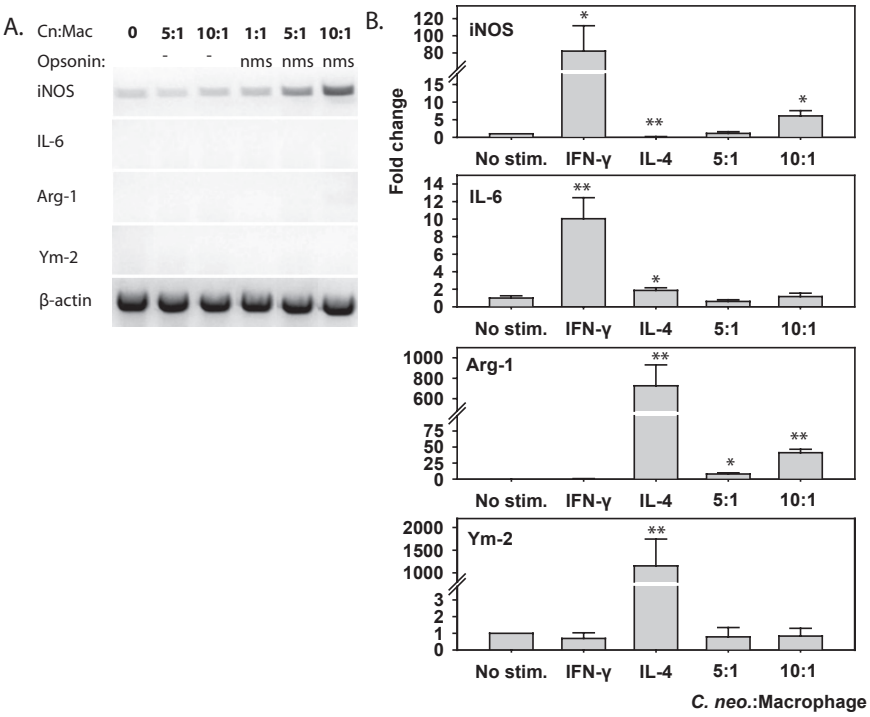

FIG 2 Interaction with encapsulated *C. neoformans* cells is insufficient to drive M1-type polarization of RAW macrophages. *C. neoformans* yeast cells were rinsed thoroughly and opsonized with normal mouse serum (NMS) or left unopsonized. Wild-type *C. neoformans* cells were then fed to RAW macrophages (A) or BMM (B) at 1, 5, or 10 yeast cells per macrophage, as indicated. Twenty-four hours later, macrophage mRNA was harvested and subsequently analyzed for the indicated M1 or M2 marker genes by RT-PCR and gel electrophoresis (A) or qPCR (B). Data in panel A are representative images from three independent experiments. Data in panel B are data combined from 6 experiments. *, $P < 0.05$, and **, $P < 0.005$, in comparisons between the indicated data and the unstimulated control. Note that the macrophages stimulated with *C. neoformans* only weakly upregulate polarization genes.

interaction between unopsonized or serum-opsonized *C. neoformans* and macrophages was insufficient to induce robust M1 or M2 polarization *in vitro*.

***Cryptococcus neoformans*-stimulated macrophages can be converted to M1/M2 polarization by *in vitro* IFN-γ/IL-4 stimulation.** Direct sensing of *C. neoformans* by macrophages *in vitro* resulted in very weak macrophage polarization (Fig. 2), while macrophages in *C. neoformans*-infected lungs were found to be strongly M2 polarized *in vivo* at weeks 1 and 2 (Fig. 1), suggesting that direct *C. neoformans*-mediated polarization is not the major driver of local immune polarization in the infected lungs and that other signals are likely to be important. As secreted cytokines are a major factor in immune polarization, the ability of cytokines to modulate *C. neoformans*-mediated polarization *in vitro* was evaluated. Macrophages were stimulated with live serum-opsonized *C. neoformans* for 24 h and then subsequently stimulated with cytokines. Results show that IL-4 cytokine signaling modulates the *C. neoformans*-induced polarization, as macrophages stimulated with *C. neoformans* followed by IL-4 (right four lanes of Fig. 3A) expressed an M2 polarization pattern with high Arg-1 and low iNOS expression which was similar to the polarization pattern displayed by control cells stimulated with IL-4 alone (left two lanes of Fig. 3A). *C. neoformans* stimulation appeared not to influence the IFN-γ-induced response; the cells stimulated first with *C. neoformans* and then with IFN-γ (right four lanes of Fig. 3B) expressed uniformly high levels of iNOS compared to those of control cells stimulated with IFN-γ alone (left two lanes of Fig. 3B). Thus, macrophages could change their weak polarization state induced by *C. neoformans* alone to a profoundly M1- or M2-polarized state under cytokine stimulation, demonstrating that exogenous cytokine signal can dominate the direct effects of the microbe on *in vitro* macrophage polarization status.

Arg-1, YM-2, and iNOS mRNA expression precisely reflects the overall polarization status. To further evaluate modulation of macrophage polarization, cytokine stimulatory conditions were first established to fully polarize macrophages *in vitro* to M1 or M2. Twenty-four hours of IFN-γ stimulation increased both iNOS and IL-6 expression and decreased mannose receptor mRNA expression below the baseline expression in RAW macrophage cultures (Fig. 4A). In contrast, 24 h of IL-4 stimulation increased Arg-1, mannose receptor, and Fizz expression (Fig. 4A). These data indicate that these culture conditions resulted in complete M1 and M2 polarization following the treatment with IFN-γ and IL-4, respectively (7, 9, 26).

The extent of M1 polarization by IFN-γ and M2 polarization by IL-4 was further confirmed at the protein expression level. Macrophages were stimulated with IFN-γ or IL-4 or left unstimulated, and culture supernatants were examined for secretion of the M1-associated cytokine tumor necrosis factor alpha (TNF-α). Cul-

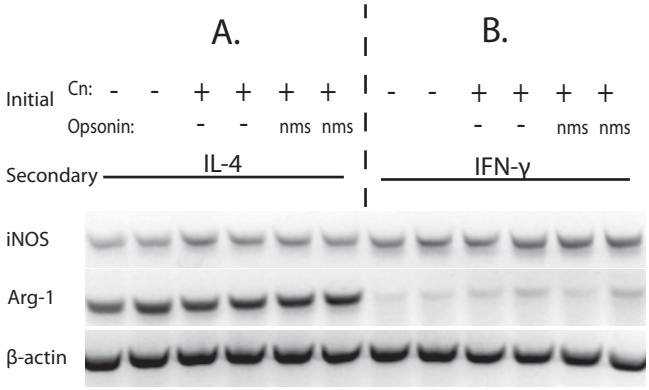

FIG 3 *Cryptococcus*-mediated polarization is superseded by exogenous cytokine signals *in vitro*. RAW macrophages were first pulsed with NMS-opsonized (right two lanes of each panel) or unopsonized *C. neoformans* (middle two lanes) or no particle controls (left two lanes) and incubated for 24 h and then stimulated with IL-4 (A) or IFN-γ (B) for a second 24-h period. The mRNA expression for iNOS (M1) or Arg-1 (M2) was analyzed by RT-PCR. Data are representative images from three independent experiments. Note that *C. neoformans*-mediated polarization can be superseded by subsequent IL-4 signaling.

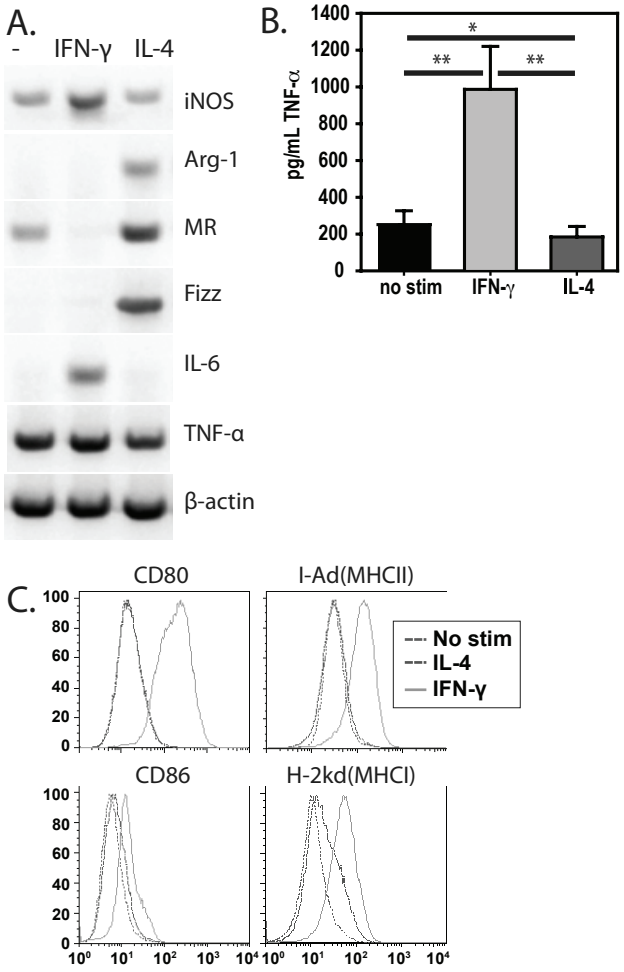

FIG 4 IFN-γ and IL-4 stimulation of RAW macrophages *in vitro* results in gene transcription, protein expression, and surface antigen expression consistent with polarized M1 versus M2 profiles. RAW macrophages were stimulated with 100 ng/ml IFN-γ or 20 ng/ml IL-4 or cultured in control medium (no stim) for 24 h. The expression of the indicated genes was measured by RT-PCR (A) or flow cytometry (C), while TNF-α secretion of the RAW cells was measured by ELISA using the culture supernatants (B). Note that "MR" in panel A refers to expression of mannose receptor (CD206), and panels A and C are representative data from three independent experiments. The data in panel B are cumulative, with $n > 20$ experimental replicates. *, $P < 0.05$; **, $P < 0.005$.

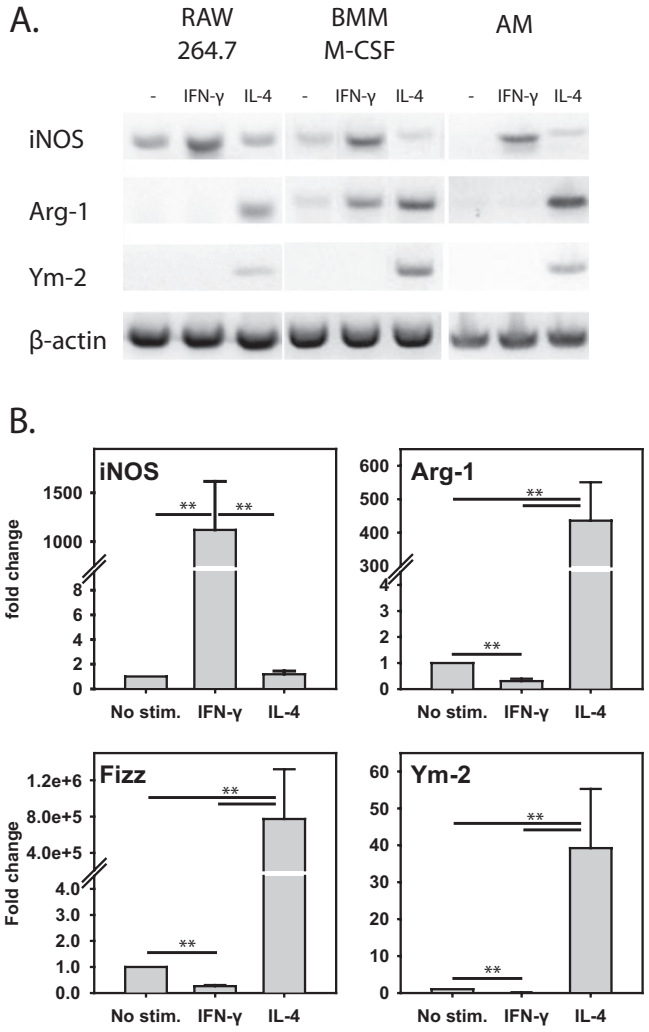

FIG 5 Cytokine stimulation induces similar changes in M1 and M2 gene induction in RAW murine macrophage cell line and primary macrophage cultures. (A) RAW 264.7 cell line macrophages (RAW 264.7), M-CSF-differentiated bone marrow-derived macrophages (BMM M-CSF), and primary alveolar macrophages (AM) were stimulated with 100 ng/ml IFN-γ or 20 ng/ml IL-4 or left unstimulated (−) for 24 h. mRNA was harvested from cells and analyzed by RT-PCR. Note that all these macrophage types responded to IFN-γ by increased iNOS expression and to IL-4 by inducing Arg-1 and Ym-2, consistent with M1 and M2 polarization, respectively. Data are representative images from three independent experiments. (B) M-CSF BMM were stimulated, and mRNA was harvested. Gene expression was analyzed quantitatively using qPCR and expressed as fold change. Error bars in panel B represent SEMs from data pooled from 6 experiments. *, $P < 0.05$; **, $P < 0.005$.

tures stimulated with IFN-γ secreted high levels of TNF-α, while those stimulated with IL-4 or left unstimulated did not (Fig. 4B). Note that the observed differences in TNF-α secretion (Fig. 4B) are much greater than the observed changes in mRNA (Fig. 4A), which is consistent with previously published data indicating posttranscriptional regulation as the rate-limiting step for TNF-α secretion (32–35). The final confirmation was performed by analysis via flow cytometry, in which macrophages stimulated with IFN-γ showed substantial upregulation of major histocompatibility complex class I (MHC-I), MHC-II, and CD80, all cell surface markers for M1 polarization in murine macrophages (10) (Fig. 4C). Thus, incubation of macrophages in IFN-γ or IL-4 for 24 h resulted in complete *in vitro* M1 or M2 polarization, respectively.

Cytokine-induced macrophage polarization patterns are similar between macrophage types. To verify that these *in vitro* effects follow the same pattern in different types of macrophages, the RAW macrophage cell line, macrophage colony-stimulating factor (M-CSF)-differentiated BMM, and primary isolated mouse alveolar macrophages were stimulated with IFN-γ or IL-4 or left unstimulated, and gene expression patterns were compared. The resting gene expression patterns were largely similar between cell types; each of the macrophage subsets had a minimal difference in a baseline expression of iNOS, Arg-1, and Ym-2 (Fig. 5A). While resting alveolar macrophages expressed no detectable iNOS, resting RAW cells and, to a lesser degree, BMM expressed a low but detectable level of iNOS (Fig. 5A). Stimulation with IFN-γ for 24 h

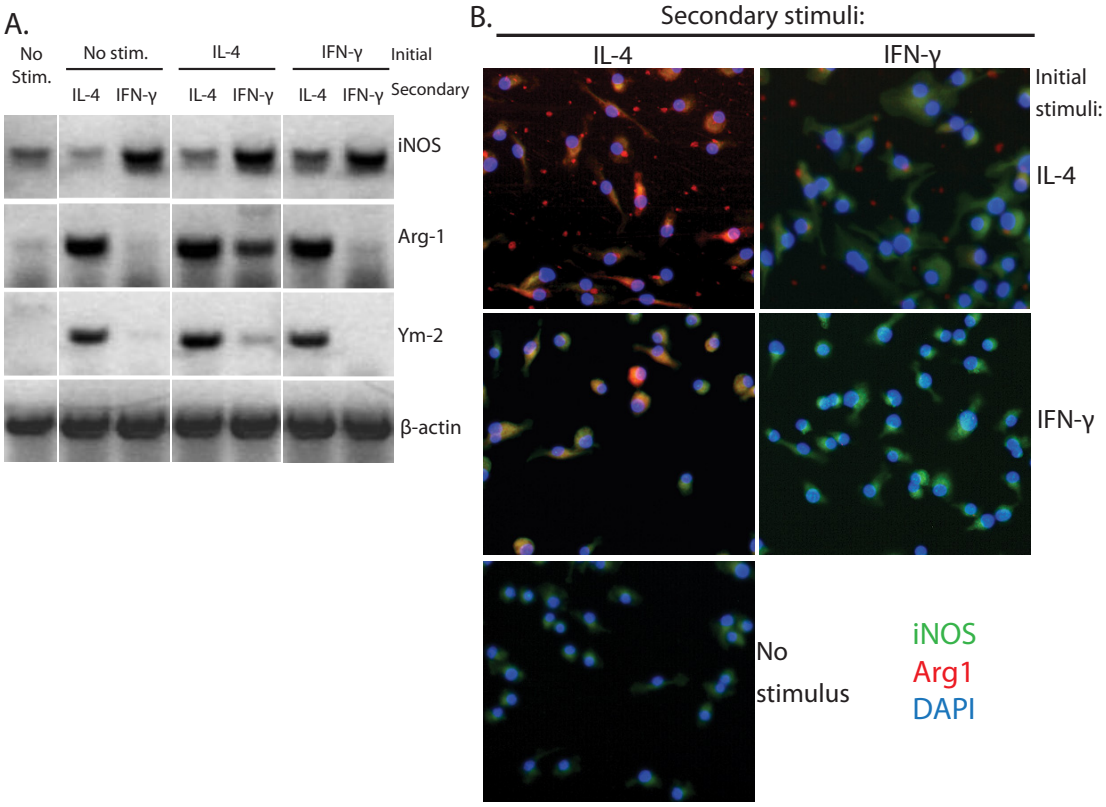

FIG 6 Cytokine-induced M1 versus M2 macrophage polarization profiles are plastic and thus reflect the most recent stimulus. RAW macrophages were incubated with the indicated primary stimulus, either IL-4 or IFN-γ, or no stimulus for 24 h. Cultures were then split and stimulated with the indicated secondary stimulus, IL-4 or IFN-γ. After 24 h of secondary stimulation, cells were harvested and mRNA was collected and analyzed for the indicated genes by RT-PCR (A) or fixed and stained with antibodies specific for iNOS and Arg-1 (B). Note that gene expression in all the assayed cultures more closely resembled cells stimulated only with the last (second) stimulus than those cultures stimulated only with the first stimulus. Data are representative images of three (A) or two (B) independent experiments.

increased iNOS expression in all types of macrophage without induction of Arg-1 or Ym-2, consistent with M1 polarization (Fig. 5A). Macrophages stimulated with IL-4 exhibited baseline or reduced iNOS expression and induced Arg-1 and Ym-2, consistent with M2 polarization (Fig. 5A). These results were confirmed quantitatively by analyzing expression levels in IFN-γ- or IL-4-stimulated BMM using quantitative PCR (qPCR). IFN-γ-stimulated BMM induced the iNOS M1 marker gene, and IL-4-stimulated BMM induced the Arg-1, Fizz, and Ym-2 M2 marker genes (Fig. 5B). Thus, regardless of small differences in the baseline expression of major M1 and M2 hallmarks, all macrophage types demonstrated similar *in vitro* responses to IFN-γ and IL-4 stimulation.

Cytokine-induced macrophage polarization changes dynamically to match the changes in the cytokine environment *in vitro*. While some *in vitro* plasticity was observed in *C. neoformans*-mediated macrophage polarization followed by cytokine stimulation (Fig. 3), *C. neoformans* was not a strong inducer of macrophage polarization (Fig. 2). Thus, we examined *in vitro* polarization plasticity in a cytokine polarization model which fully polarized macrophage cultures (Fig. 4). Macrophage cultures were initially polarized to M1 or M2 with IFN-γ or IL-4 or left unstimulated for 24 h. These cultures were then divided, and each portion was stimulated with either IL-4 or IFN-γ for a second 24-h period. Independent of the initial polarization, macrophages treated with IFN-γ during the second 24-h incubation strongly upregulated iNOS, while the expression of Arg-1 and Ym-2 M2 markers resembled the baseline levels (Fig. 6A). Similarly, macrophages stimulated with IL-4 upregulated the Arg-1 and Ym-2 M2 marker genes, regardless of their initial M1 or M2 polarization (Fig. 6A). Thus, macrophages respond to changes in cytokine environment *in vitro* by altering their mRNA expression of M1/M2 marker genes.

To confirm these outcomes at a protein level and to determine if the changes in protein expression have occurred uniformly across the entire macrophage population, cells were sequentially stimulated as described for Fig. 4A and examined by immunofluorescence microscopy with antibodies specific for Arg-1 and iNOS. Consistent with mRNA expression outcomes (Fig. 6A), cells stimulated second with IL-4 expressed higher Arg-1 levels (Fig. 6B, left side, red), while those stimulated second with IFN-γ expressed higher levels of iNOS (Fig. 6B, right side, green), independent of initial stimulation. Of note, staining levels were uniform in most cells within the same condition, indicating that the mRNA expression patterns measured in Fig. 4A resulted from changes across the entire populations and not increased expression of M1 and M2 genes each in a different cell subset. Thus, *in vitro* cytokine-induced macrophage polarization can be reversed in the same cell, resulting in M1 or M2 polarization that reflects

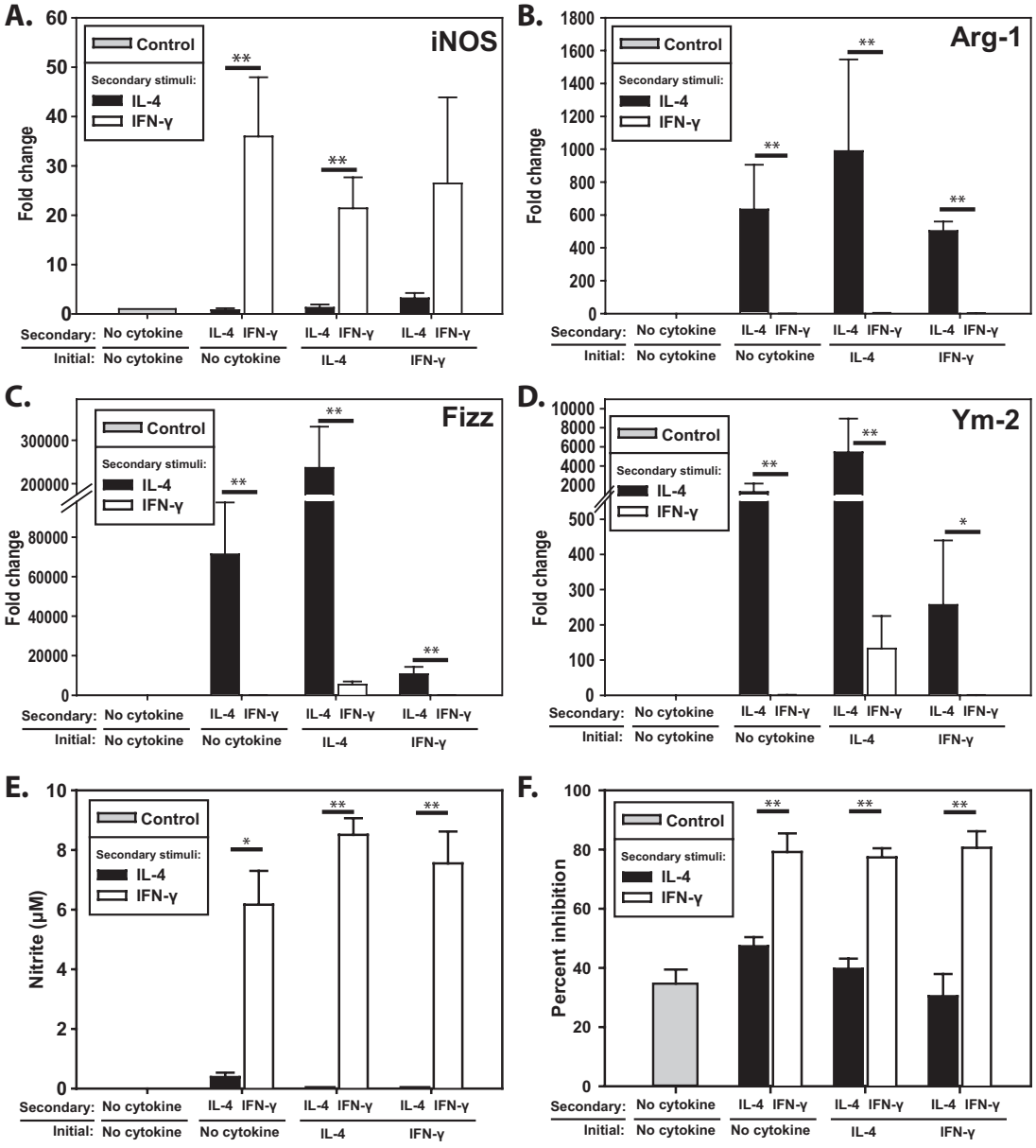

FIG 7 M1 versus M2 polarization plasticity *in vitro* is reflected by fungicidal activity of macrophages. BMM were stimulated for 24 h with IL-4 or IFN-γ or left unstimulated. These cultures were divided into subgroups and restimulated with IL-4 or IFN-γ. After 24 h of secondary stimulation, cells were harvested, and mRNA was collected and analyzed for the indicated genes by qPCR (A to D) or BMM were then incubated with NMS-opsonized *C. neoformans*. After another 24 h, the culture supernatants were reserved and analyzed for nitric oxide production by Griess reaction E, and the yeast cells were collected by lysing the macrophages and enumerated (F). In panel F, the data on the *y* axis is the percent inhibition calculated as described in Materials and Methods. Error bars represent SEMs. Graphs in panels A to F are cumulative from 6 experiments. Note that raw CFU data from each independent experiment in panel F displayed statistically significant *P* values between the comparisons, which are noted in panel F. *, $P < 0.05$; **, $P < 0.005$.

the most recent signaling environment rather than any initially acquired macrophage polarization status.

Plasticity of M1 versus M2 macrophage polarization is reflected by quantitative changes in gene expression and macrophage fungicidal activity. M1-polarized macrophages inhibit *C. neoformans* growth more efficiently than resting or M2-polarized macrophages (7–9, 14, 15, 19, 22). Our final goal was to evaluate if plastic changes in macrophage polarization phenotype translated into corresponding fungicidal activity *in vitro*. To increase translational value of this model, macrophage polarization plasticity was tested in BMM. M1/M2 marker gene mRNA expression levels were analyzed quantitatively from BMM stimulated sequentially with IFN-γ or IL-4 as described for Fig. 6. Macrophages stimulated second with IFN-γ expressed higher iNOS levels, while macrophages stimulated second with IL-4 expressed high levels of the Arg-1, Fizz, and Ym-2 M2 marker genes (Fig. 7A to D). These data are consistent with Fig. 6 and support the plasticity of primary macrophage polarization.

Lastly, we extended our studies of macrophage polarization plasticity to measurements of fungicidal activity. Macrophages

were sequentially stimulated as described for Fig. 6 and 7A and then pulsed with live *C. neoformans*. Consistent with Fig. 7A to D, macrophages stimulated second with IFN-γ produced dramatically more nitric oxide than unstimulated cells or those stimulated second with IL-4, again independent of any initial stimulus (Fig. 7E). The microbial growth inhibition by macrophages was measured at 24 h relative to yeast growth in medium alone. Independent of any previous stimulation, macrophages with secondary IFN-γ stimulation inhibited yeast growth more efficiently than those with secondary IL-4 treatment (Fig. 7F). Furthermore, all cultures treated last with IFN-γ showed equally high levels of fungal inhibition, while all the cultures treated last with IL-4 showed equally low fungicidal activity comparable to that of nonstimulated macrophages. Thus, macrophages display microbicidal plasticity in response to changes in the external cytokine milieu *in vitro* and in concert with the corresponding changes in M1/M2 marker gene expression.

DISCUSSION

These data, for the first time, demonstrate that *in vitro* macrophages are capable of complete repolarization from M2 to M1 and vice versa in response to changes in the cytokine environment. These changes in macrophage polarization are rapid and occur at the levels of gene expression, protein, metabolite, and microbicidal activity. We also show that the cytokine environment reverses the direct effect of *C. neoformans* on macrophage polarization, indicating that extrinsic factors, such as cytokines, are stronger in driving macrophage polarization than direct interactions with the microbe itself. This information has important implications for understanding the mechanisms of clearance versus long-term persistence of *C. neoformans* infection and could be applicable for the development of new therapeutic strategies.

Although clearance of *C. neoformans* depends on the development of protective T-cell-mediated immunity, macrophages are the distal effectors, which either execute fungicidal function or promote intracellular persistence of *C. neoformans*. It has been widely accepted that M1-polarized macrophages are effective fungicidal cells, while M2 macrophages are not (7–9, 22, 30, 36). Previous studies suggested that macrophages remain responsive to sequential cytokine signals (37). Our novel data now clearly demonstrate that a complete plastic reversal of macrophage polarization from M2 to M1 and vice versa is possible. Initial, 24-h stimulation with IFN-γ or IL-4 *in vitro* resulted in complete M1 or M2 polarization, respectively, as evidenced by uniform induction of the applicable marker genes (Fig. 4) and by the induction of fungistatic ability in the M1-polarized macrophages but not in the M2 cells. The latter point is evidenced by the macrophages stimulated with IFN-γ or IL-4 alone (Fig. 7E and F; bars with "no cytokine" listed as initial stimulation). This initial polarization was completely reversed after secondary stimulation using the opposite polarizing cytokine (Fig. 6 and 7), as gene expression was consistent with the secondary polarizing cytokine and independent of initial stimulus. More importantly, reversal of marker genes was accompanied by the total reversal of macrophage fungistatic potential (Fig. 7F), verifying that polarization reversal was complete. This is the first published evidence that macrophage polarization plasticity extends to microbicidal activity (Fig. 7F). This is especially relevant, as microbicidal activity was the original defining characteristic of activated macrophages (20, 21, 38), later termed classically activated or M1 macrophages.

Our previous study demonstrated that macrophage M1/M2 polarization status in the lungs can evolve during the course of cryptococcal infection, mimicking the published changes in lung cytokine profiles (23). However, it is unknown whether overall polarization of lung macrophages can be achieved without "repopulation" of the infected lungs with new cells from blood monocytes. Our data show that M1/M2 polarization status can be rapidly induced and completely reversed within 24 h, by exchanging M2 with M1-driving cytokines and vice versa. This rapid reversal of macrophage polarization *in vitro* suggests that lung macrophage polarization is highly plastic, and thus the cells are likely to rapidly repolarize without the need to be replaced by newly arriving cells. The analysis of macrophage polarization status performed *in vivo* in a BALB/c mouse model (Fig. 1) shows that macrophage polarization changes throughout the entire course of cryptococcal infection from baseline to M2 during early infection and then to M1 during late infection. Earlier studies in this model demonstrated that Ly6C^{high} monocytes are recruited and mature into exudate macrophages during the first 2 to 3 weeks. Their recruitment peaks at day 14 postinfection and tapers significantly after that, resulting in only a minor late recruitment (10). Based on the comparisons of the recruitment and lung macrophage polarization kinetics *in vivo* and how rapidly and uniformly repolarization of macrophages can occur in response to changing cytokine environment, our data favor the hypothesis that macrophages repolarize *in vivo* without cell-by-cell replacement.

While the results presented here show that *in vitro* macrophages can rapidly repolarize when presented with dynamic changes in cytokine concentrations, macrophage polarization can result from a variety of other interactions, such as with other cells through direct cell-to-cell contact as well as lipid mediators and other protein cytokines. Thus, we speculate that repolarization of lung macrophages *in vivo* is influenced by many factors beyond the cytokines studied here. Macrophage polarization may well be plastic to these additional polarizing factors, but future studies are required to elucidate this point.

Macrophage polarization plasticity has important therapeutic implications. This work shows that even profoundly M2-skewed macrophages can be repolarized into fungicidal M1 macrophages. Thus, putative treatments which would reverse M2 to M1 polarization in the *C. neoformans*-infected lung are likely to be beneficial. Conversely, these data reinforce the importance of pathogen-mediated immune modulation, as virulence factors expressed by *C. neoformans* can lead to immune bias that polarizes macrophages toward M2 (11, 18, 39). Depending on the strengths of these interactions, *C. neoformans* can promote its early virulence, support its long-term persistence, or overcome any insufficient M1-polarizing signals. Therapeutically reprograming macrophages into M1 cells would be especially beneficial in these circumstances.

In summary, this study has identified that macrophages are highly responsive in terms of altering their polarization pattern, both *in vivo* and *in vitro*. These effects extended to microbicidal effects of macrophages, suggesting that future therapeutic strategies gauged to reprogram macrophages to M1 polarization could be a feasible way to improve management of *C. neoformans* infections.

MATERIALS AND METHODS

Culture and opsonization of *Cryptococcus neoformans* yeast. *Cryptococcus neoformans* cultures were grown while being shaken at 37°C for 4 days in Sabouraud dextrose broth (1% neopeptone, 2% dextrose; Difco, Detroit, MI) as described previously (10, 26). Yeast cells were rinsed in sterile saline and then enumerated by a hemocytometer. Yeast preparations for all infections, *in vivo* or *in vitro*, were serially diluted and plated onto Sabouraud dextrose agarose plates, and colonies were counted after 48 h to confirm infectious dose.

***In vivo* intratracheal infection.** BALB/c mice were purchased from Jackson Laboratory (Bar Harbor, ME). Animal housing and procedures were all approved by the VA institutional animal case and use committees. Mice were infected intratracheally as previously described (10, 11, 26, 39). Briefly, mice were anesthetized with ketamine (100 mg/kg of body weight) and xylazine (6.8 mg/kg) and immobilized on a surgical board. Under sterile technique, the trachea was exposed by incision and then inoculated with 10,000 *C. neoformans* cells (ATCC 24067; Manassas, VA) in 30 μl sterile saline using a 30-gauge needle. The surgical wound was closed with cyanoacrylate adhesive, and the mice recovered under thermal support. Four mice were infected for each time point, and all mice survived anesthesia and recovered from surgery.

Macrophage isolation. At the indicated time points following infection, mice were sacrificed and their lungs were perfused and collected. Single-cell suspensions of leukocytes were isolated from lungs by enzymatic digestion as previously described (10, 26). Macrophages were selected from digested lung samples by 90-min adherence selection on tissue culture plastic. Nonadherent cells were rinsed away, and the remaining macrophages were collected in Trizol reagent.

mRNA purification. *Ex vivo* and *in vitro* macrophages were lysed in Trizol reagent (Life Technologies, Inc., Gaithersburg, MD), and subsequent isolation of mRNA was conducted as previously described (26). Purified mRNA was resuspended in RNase-free water, and the concentration was measured using a spectrophotometer.

Reverse transcriptase PCR. Reverse transcription was performed using the Access reverse transcriptase PCR (RT-PCR) system (Promega, Madison, WI) as per the manufacturer's instructions. These procedures were utilized previously (26).

Real-time PCR. For real-time quantitative PCR (qPCR), mRNA was reverse transcribed into cDNA using the QuantiTect reverse transcription kit from Qiagen (Valencia, CA) according to the manufacturer's instructions. Expression levels were measured using primers purchased from Life Technologies, Inc. (Gaithersburg, MD): arginase sense, CAGAAGAATG GAAGAGTCAG; arginase antisense, CAGATATGCAGGGAGTCACC; Fizz sense, GGTCCCAGTGCATATGGATGAGACCATAGA; Fizz antisense, CACCTCTTCACTCGAGGGACAGTTGGCAGC; IL-6 sense (RT-PCR only), GACAAAGCCAGAGTCCTTCAGAGAG; IL-6 antisense (RT-PCR only), CTAGGTTTGCCGAGTAGATCTC; IL-6 sense (qPCR only), GAGGATACCACTCCCAACAGACC; IL-6 antisense (qPCR only), AAGTGCATCATCGTTGTTCATACA; iNOS sense, TTTGCTTCCATG CTAATGCGAAAG; iNOS antisense, GCTCTGTTGAGGTCTAAAGGC TCCG; TNF-α sense, CCTGTAGCCCACGTCGTAGC; TNF-α antisense, AGCAATGACTCCAAAGTAGACC; Ym-2 sense, CAGAACCGTCAGAC ATTCATTA; Ym-2 antisense, ATGGTCCTTCCAGTAGGTAATA; β-actin sense, TGGAATCCTGTGGCATCCATGAAAC; β-actin sense, TAAAACGCAGCTCAGTAACAGTCCG; GAPDH sense, TATGTCGTG GAGTCTACTGGT; and GAPDH antisense, GAGTTGTCATATTTCT CGT. Note that all primer sequences are listed 5′ to 3′ and were used in previously published works (10, 26, 40) except for the IL-6 qPCR primers. qPCR reactions used Power SYBR green PCR master mix (Life Technologies, Inc., Gaithersburg, MD) using the manufacturer's instructions. Reactions were temperature cycled, and SYBR green levels were measured using an Mx3000P system (Stratagene, La Jolla, CA). The cycling parameters were as follows: 95°C for 15 s, 60°C for 30 s, and then 72°C for 30 s for a total of 40 cycles. Note that for all qPCR, signally stimulated cells (IFN-γ alone or IL-4 alone) are assayed along with the experimental sequentially stimulated conditions as positive-control M1 or M2 marker gene expression, respectively. Expression values were standardized to GAPDH expression. Data from the *in vivo* experiment was displayed as percent GAPDH. In order to combine *in vitro* experimental repeats, it was necessary to normalize the data to the control conditions indicated in the figure legends by dividing the experimental percent GAPDH values by the control to calculate "fold change."

Bone marrow-derived macrophage culture. BMM were cultured as previously described (26). Briefly, BALB/c mice were euthanized consistent with established animal care protocols approved by the VA institutional animal case and use committees. Tibias and femurs were excised, and marrow cells were flushed and dispersed into culture medium. Marrow cells were cultured in Dulbecco's minimal essential medium (DMEM) containing 20% fetal calf serum, GlutaMAX, MEM-nonessential amino acids, sodium pyruvate, penicillin, and streptomycin (all purchased from Life Technologies, Inc., Gaithersburg, MD) and 50 ng/ml recombinant murine M-CSF (PeproTech, Rocky Hill, NJ) for seven days. Ten additional milliliters of the above-described medium was added once on the fourth day of culture. For subsequent experiments, BMM were removed from differentiation dishes using cold sterile pyrogen-free phosphate-buffered saline (PBS) (Life Technologies, Inc., Gaithersburg, MD) and subsequently cultured in RPMI 1640 (Life Technologies, Inc., Gaithersburg, MD) containing 10% fetal calf serum, GlutaMAX, MEM-nonessential amino acids, sodium pyruvate, and 5 ng/ml M-CSF. Note that this 5 ng/ml M-CSF was included in all BMM stimulation and infection cultures.

RAW culture. RAW 264.7 macrophage-like cells (ATCC, Manassas, VA) were cultured as previously described in DMEM (Life Technologies, Inc., Gaithersburg, MD) with 10% fetal calf serum (Life Technologies, Inc., Gaithersburg, MD) and penicillin and streptomycin (Life Technologies, Inc., Gaithersburg, MD) (26). Cultures were split 1:5 every other day. Cells were removed from plates by gentle scraping in fresh medium and counted by hemocytometer.

***In vitro* stimulation of macrophages with *C. neoformans*.** *C. neoformans* cells were cultured, rinsed, and enumerated as described above. For some *in vitro* conditions, *C. neoformans* strain H99 (ATCC 208821; Manassas, VA) were opsonized in 10% normal mouse serum (Innovative Research, Novi, MI) at 37°C for 45 min. For stimulation with *C. neoformans* RAW macrophages or BMM, 1×10^6 macrophages were plated into each well of a 24-well tissue culture plate. Macrophages were infected with 1×10^6, 5×10^6, or 10×10^6 opsonized or 5×10^6 or 10×10^6 unopsonized *C. neoformans* cells (for 1:1, 5:1, or 10:1 yeast per macrophage) for 3 h, and then extracellular yeast was washed away. Cultures were incubated for 24 additional hours and then harvested in Trizol as described above or restimulated with 100 ng/ml IFN-γ (PeproTech, Rocky Hill, NJ) or 20 ng/ml IL-4 (PeproTech, Rocky Hill, NJ) and then harvested into Trizol after a second 24-h period.

Cytokine stimulation. Culture medium on RAW macrophages or BMM was replaced with fresh medium, resulting in a final concentration of 100 ng/ml IFN-γ or 20 ng/ml IL-4, and cultured for 24 h. Cultures were split, replated at 1×10^6 cells per well in a 24-well plate, and secondarily stimulated with IFN-γ- or IL-4-containing medium for a second 24-h period. At time of harvest, supernatants were reserved for enzyme-linked immunosorbent assay (ELISA) and cells were collected for flow cytometry, RT-PCR, qPCR, or immunofluorescence.

TNF-α ELISA. TNF-α secreted from supernatant collected from stimulated RAW macrophages was measured using mouse TNF-α ELISA MAX standard system (BioLegend, San Diego, CA) using the manufacturer's protocol.

Flow cytometry. Stimulated RAW macrophages were removed from wells and incubated in mouse BD Fc Block (BD Biosciences, San Jose, CA) for 30 min on ice. Samples were divided and aliquots stained using anti-CD80-phycoerythrin (PE) and anti-CD86-fluorescein isothiocyanate (FITC) or anti-I-A^d-PE and anti-H-$2K^d$-FITC antibodies (all purchased from BD Biosciences, San Jose, CA). Note that expression of these surface

proteins is considered a marker for M1 polarization of macrophages. Compensation for spectral mixing was applied through flow cytometric analysis of cells singly stained with antibodies against CD45 with either PE or FITC. Flow cytometry was performed using a FACS LSR2 flow cytometer.

Immunofluorescence. RAW macrophages were plated onto glass coverslips at 5×10^5 cells per well on sterile coverslips contained in the wells of 6-well plates and then sequentially stimulated with IFN-γ and IL-4 as described above. After the last stimulation, cells were fixed with 2% paraformaldehyde in PBS, permeabilized with 0.1% Triton X-100, blocked and stained with anti-iNOS antibody conjugated to FITC, anti-arginase antibody conjugated to Alexa Fluor 546 (both from Imgenex, San Diego, CA), and DAPI (4′,6-diamidino-2-phenylindole) as described in reference 26. Images were acquired using a Zeiss LSM510 confocal microscope using the appropriate filters.

Fungicidal activity of macrophages. BMM were sequentially stimulated as described above and plated at 1×10^6 cells per well and then infected with 25,000 CFU of normal mouse serum (NMS)-opsonized *C. neoformans* strain H99. Cocultures were harvested after 24 h by centrifugation of the culture plates. Supernatants were reserved and analyzed for nitric oxide by Griess reaction (41, 42). The pellet including the extracellular and intracellular yeasts was liberated by lysing the macrophages in sterile water. The number of *C. neoformans* CFU was determined by plating 10-fold serial dilutions for each sample onto Sabouraud dextrose agar plates. Colonies were counted after 48 h, and the total number of *C. neoformans* CFU was calculated from colony count and dilution. Percent inhibition was calculated by dividing the CFU for each well by the average CFU in wells without macrophages and then subtracting this from 1 and multiplying the result by 100. Note that yeast cell phagocytosis was observed to be similar and relatively low in all macrophage conditions (unpolarized versus M1 versus M2), consistent with previously published results (43, 44). Thus, most yeast cells resided in the medium during this assay, suggesting that the observed inhibition of yeast growth may involve intracellular and extracellular mechanisms.

Statistics. Graphs represent arithmetic means ± standard errors of the means (SEMs). For statistical analysis of data, normality and equality of variance of data sets were determined by the Shapiro-Wilk and Levene median test, respectively. Those data sets which were normal and had equal variance were compared by Student's *t* test. Note that the percent inhibition data (Fig. 7F) and nitric oxide detection data (Fig. 7E) met these criteria. The ELISA data (Fig. 4B) and the combined qPCR (Fig. 5B and 7A to D) were not normal and were thus analyzed by Mann-Whitney rank sum tests. All statistical tests were calculated using SigmaPlot software (Systat Software Inc., San Jose, CA). Significance levels of these tests are indicated in the figure legends. *, $P < 0.05$; **, $P < 0.005$.

ACKNOWLEDGMENTS

This project was funded by a VA merit grant (1I01BX000656-01A1; M.A.O.). M.J.D. was supported by the Multidisciplinary Training Program in Pulmonary Diseases (PHS T32-HL07749-19).

We thank John Osterholzer for his helpful comments regarding this work and acknowledge the assistance of Rebekah Chapman, Antoni Malachowski, Jacob Carolan, Zachary Hadd, Daniel Lyons, and Priya Vedula under the auspices of Undergraduate Research Opportunity Program at University of Michigan.

REFERENCES

1. **Chuck SL, Sande MA.** 1989. Infections with *Cryptococcus neoformans* in the acquired immunodeficiency syndrome. N. Engl. J. Med. **321:**794–799.
2. **Jarvis JN, Harrison TS.** 2007. HIV-associated cryptococcal meningitis. AIDS **21:**2119–2129.
3. **Park BJ, Wannemuehler KA, Marston BJ, Govender N, Pappas PG, Chiller TM.** 2009. Estimation of the current global burden of cryptococcal meningitis among persons living with HIV/AIDS. AIDS **23:**525–530.
4. **Baddley JW, Perfect JR, Oster RA, Larsen RA, Pankey GA, Henderson H, Haas DW, Kauffman CA, Patel R, Zaas AK, Pappas PG.** 2008. Pulmonary cryptococcosis in patients without HIV infection: factors associated with disseminated disease. Eur. J. Clin. Microbiol. Infect. Dis. **27:**937–943.
5. **Hofman V, Venissac N, Mouroux C, Butori C, Mouroux J, Hofman P.** 2004. Disseminated pulmonary infection due to *Cryptococcus neoformans* in a non immunocompromised patient. Ann. Pathol. **24:**187–191.
6. **Chen J, Varma A, Diaz MR, Litvintseva AP, Wollenberg KK, Kwon-Chung KJ.** 2008. Cryptococcus neoformans strains and infection in apparently immunocompetent patients, China. Emerg. Infect. Dis. **14:** 755–762.
7. **Arora S, Hernandez Y, Erb-Downward JR, McDonald RA, Toews GB, Huffnagle GB.** 2005. Role of IFN-gamma in regulating T2 immunity and the development of alternatively activated macrophages during allergic bronchopulmonary mycosis. J. Immunol. **174:**6346–6356.
8. **Hardison SE, Ravi S, Wozniak KL, Young ML, Olszewski MA, Wormley FL, Jr..** 2010. Pulmonary infection with an interferon-gamma-producing *Cryptococcus neoformans* strain results in classical macrophage activation and protection. Am. J. Pathol. **176:**774–785.
9. **Zhang Y, Wang F, Tompkins KC, McNamara A, Jain AV, Moore BB, Toews GB, Huffnagle GB, Olszewski MA.** 2009. Robust Th1 and Th17 immunity supports pulmonary clearance but cannot prevent systemic dissemination of highly virulent *Cryptococcus neoformans* H99. Am. J. Pathol. **175:**2489–2500.
10. **Osterholzer JJ, Chen GH, Olszewski MA, Zhang YM, Curtis JL, Huffnagle GB, Toews GB.** 2011. Chemokine receptor 2-mediated accumulation of fungicidal exudate macrophages in mice that clear cryptococcal lung infection. Am. J. Pathol. **178:**198–211.
11. **He X, Lyons DM, Toffaletti DL, Wang F, Qiu Y, Davis MJ, Meister DL, Dayrit JK, Lee A, Osterholzer JJ, Perfect JR, Olszewski MA.** 2012. Virulence factors identified by *Cryptococcus neoformans* mutant screen differentially modulate lung immune responses and brain dissemination. Am. J. Pathol. **181:**1356–1366.
12. **MacMicking J, Xie QW, Nathan C.** 1997. Nitric oxide and macrophage function. Annu. Rev. Immunol. **15:**323–350.
13. **Nauseef WM.** 2008. Biological roles for the NOX family NADPH oxidases. J. Biol. Chem. **283:**16961–16965.
14. **Granger DL, Hibbs JB, Jr, Perfect JR, Durack DT.** 1988. Specific amino acid (L-arginine) requirement for the microbiostatic activity of murine macrophages. J. Clin. Invest. **81:**1129–1136.
15. **Alspaugh JA, Granger DL.** 1991. Inhibition of *Cryptococcus neoformans* replication by nitrogen oxides supports the role of these molecules as effectors of macrophage-mediated cytostasis. Infect. Immun. **59:** 2291–2296.
16. **Herbert DR, Hölscher C, Mohrs M, Arendse B, Schwegmann A, Radwanska M, Leeto M, Kirsch R, Hall P, Mossmann H, Claussen B, Förster I, Brombacher F.** 2004. Alternative macrophage activation is essential for survival during schistosomiasis and downmodulates T helper 1 responses and immunopathology. Immunity **20:**623–635.
17. **Anthony RM, Urban JF, Jr, Alem F, Hamed HA, Rozo CT, Boucher JL, Van Rooijen N, Gause WC.** 2006. Memory T(H)2 cells induce alternatively activated macrophages to mediate protection against nematode parasites. Nat. Med. **12:**955–960.
18. **Osterholzer JJ, Surana R, Milam JE, Montano GT, Chen GH, Sonstein J, Curtis JL, Huffnagle GB, Toews GB, Olszewski MA.** 2009. Cryptococcal urease promotes the accumulation of immature dendritic cells and a non-protective T2 immune response within the lung. Am. J. Pathol. **174:**932–943.
19. **Voelz K, Lammas DA, May RC.** 2009. Cytokine signaling regulates the outcome of intracellular macrophage parasitism by *Cryptococcus neoformans*. Infect. Immun. **77:**3450–3457.
20. **Gordon S, Martinez FO.** 2010. Alternative activation of macrophages: mechanism and functions. Immunity **32:**593–604.
21. **Sica A, Mantovani A.** 2012. Macrophage plasticity and polarization: *in vivo* veritas. J. Clin. Invest. **122:**787–795.
22. **Müller U, Stenzel W, Köhler G, Werner C, Polte T, Hansen G, Schütze N, Straubinger RK, Blessing M, McKenzie AN, Brombacher F, Alber G.** 2007. IL-13 induces disease-promoting type 2 cytokines, alternatively activated macrophages and allergic inflammation during pulmonary infection of mice with *Cryptococcus neoformans*. J. Immunol. **179:**5367–5377.
23. **Nicola AM, Robertson EJ, Albuquerque P, Derengowski Lda S, Casadevall A.** 2011. Nonlytic exocytosis of *Cryptococcus neoformans* from macrophages occurs in vivo and is influenced by phagosomal pH. mBio **2**(4): e00167-11. http://dx.doi.org/10.1128/mBio.00167-11.

24. **Charlier C, Nielsen K, Daou S, Brigitte M, Chretien F, Dromer F.** 2009. Evidence of a role for monocytes in dissemination and brain invasion by *Cryptococcus neoformans*. Infect. Immun. **77:**120–127.
25. **Chrétien F, Lortholary O, Kansau I, Neuville S, Gray F, Dromer F.** 2002. Pathogenesis of cerebral *Cryptococcus neoformans* infection after fungemia. J. Infect. Dis. **186:**522–530.
26. **Arora S, Olszewski MA, Tsang TM, McDonald RA, Toews GB, Huffnagle GB.** 2011. Effect of cytokine interplay on macrophage polarization during chronic pulmonary infection with *Cryptococcus neoformans*. Infect. Immun. **79:**1915–1926.
27. **Traynor TR, Kuziel WA, Toews GB, Huffnagle GB.** 2000. CCR2 expression determines T1 versus T2 polarization during pulmonary *Cryptococcus neoformans* infection. J. Immunol. **164:**2021–2027.
28. **Chen GH, McNamara DA, Hernandez Y, Huffnagle GB, Toews GB, Olszewski MA.** 2008. Inheritance of immune polarization patterns is linked to resistance versus susceptibility to *Cryptococcus neoformans* in a mouse model. Infect. Immun. **76:**2379–2391.
29. **Jain AV, Zhang Y, Fields WB, McNamara DA, Choe MY, Chen GH, Erb-Downward J, Osterholzer JJ, Toews GB, Huffnagle GB, Olszewski MA.** 2009. Th2 but not Th1 immune bias results in altered lung functions in a murine model of pulmonary *Cryptococcus neoformans* infection. Infect. Immun. **77:**5389–5399.
30. **Zhang Y, Wang F, Bhan U, Huffnagle GB, Toews GB, Standiford TJ, Olszewski MA.** 2010. TLR9 signaling is required for generation of the adaptive immune protection in *Cryptococcus neoformans*-infected lungs. Am. J. Pathol. **177:**754–765.
31. **Lee A, Toffaletti DL, Tenor J, Soderblom EJ, Thompson JW, Moseley MA, Price M, Perfect JR.** 2010. Survival defects of *Cryptococcus neoformans* mutants exposed to human cerebrospinal fluid result in attenuated virulence in an experimental model of meningitis. Infect. Immun. **78:**4213–4225.
32. **Solomon KA, Covington MB, DeCicco CP, Newton RC.** 1997. The fate of pro-TNF-alpha following inhibition of metalloprotease-dependent processing to soluble TNF-alpha in human monocytes. J. Immunol. **159:**4524–4531.
33. **Black RA, Rauch CT, Kozlosky CJ, Peschon JJ, Slack JL, Wolfson MF, Castner BJ, Stocking KL, Reddy P, Srinivasan S, Nelson N, Boiani N, Schooley KA, Gerhart M, Davis R, Fitzner JN, Johnson RS, Paxton RJ, March CJ, Cerretti DP.** 1997. A metalloproteinase disintegrin that releases tumour-necrosis factor-alpha from cells. Nature **385:**729–733.
34. **Shurety W, Pagan JK, Prins JB, Stow JL.** 2001. Endocytosis of uncleaved tumor necrosis factor-alpha in macrophages. Lab. Invest. **81:**107–117.
35. **Peiretti F, Canault M, Deprez-Beauclair P, Berthet V, Bonardo B, Juhan-Vague I, Nalbone G.** 2003. Intracellular maturation and transport of tumor necrosis factor alpha converting enzyme. Exp. Cell Res. **285:**278–285.
36. **Hernandez Y, Arora S, Erb-Downward JR, McDonald RA, Toews GB, Huffnagle GB.** 2005. Distinct roles for IL-4 and IL-10 in regulating T2 immunity during allergic bronchopulmonary mycosis. J. Immunol. **174:**1027–1036.
37. **Stout RD, Jiang C, Matta B, Tietzel I, Watkins SK, Suttles J.** 2005. Macrophages sequentially change their functional phenotype in response to changes in microenvironmental influences. J. Immunol. **175:**342–349.
38. **Mackaness GB.** 1962. Cellular resistance to infection. J. Exp. Med. **116:**381–406.
39. **Qiu Y, Davis MJ, Dayrit JK, Hadd Z, Meister DL, Osterholzer JJ, Williamson PR, Olszewski MA.** 2012. Immune modulation mediated by cryptococcal laccase promotes pulmonary growth and brain dissemination of virulent *Cryptococcus neoformans* in mice. PLoS One **7:**e47853. http://dx.doi.org/10.1371/journal.pone.0047853.
40. **Martinon F, Chen X, Lee AH, Glimcher LH.** 2010. TLR activation of the transcription factor XBP1 regulates innate immune responses in macrophages. Nat. Immunol. **11:**411–418.
41. **Tsang AW, Oestergaard K, Myers JT, Swanson JA.** 2000. Altered membrane trafficking in activated bone marrow-derived macrophages. J. Leukoc. Biol. **68:**487–494.
42. **Granger DL, Taintor RR, Boockvar KS, Hibbs JB, Jr..** 1996. Measurement of nitrate and nitrite in biological samples using nitrate reductase and Griess reaction. Methods Enzymol. **268:**142–151.
43. **Cross CE, Collins HL, Bancroft GJ.** 1997. CR3-dependent phagocytosis by murine macrophages: different cytokines regulate ingestion of a defined CR3 ligand and complement-opsonized *Cryptococcus neoformans*. Immunology **91:**289–296.
44. **Collins HL, Bancroft GJ.** 1992. Cytokine enhancement of complement-dependent phagocytosis by macrophages: synergy of tumor necrosis factor-alpha and granulocyte-macrophage colony-stimulating factor for phagocytosis of *Cryptococcus neoformans*. Eur. J. Immunol. **22:**1447–1454.